Ann. Phys. (Berlin) 525, No. 7, 452–471 (2013) / DOI 10.1002/andp.201300010

annalen der physik

Review Article

Microwave and submillimeter molecular transitions and their dependence on fundamental constants

Mikhail G. Kozlov[1,2] *and Sergei A. Levshakov*[2,3,*]

Received 22 January 2013, revised 26 February 2013, accepted 18 March 2013
Published online 30 April 2013

Microwave and submillimeter molecular transition frequencies between nearly degenerated rotational levels, tunneling transitions, and mixed tunneling-rotational transitions show an extremely high sensitivity to the values of the fine-structure constant, α, and the electron-to-proton mass ratio, μ. This review summarizes the theoretical background on quantum-mechanical calculations of the sensitivity coefficients of such transitions to tiny changes in α and μ for a number of molecules which are usually observed in Galactic and extragalactic sources, and discusses the possibility of testing the space- and time-invariance of fundamental constants through comparison between precise laboratory measurements of the molecular rest frequencies and their astronomical counterparts. In particular, diatomic radicals CH, OH, NH^+, and a linear polyatomic radical C_3H in Π electronic ground state, polyatomic molecules NH_3, ND_3, NH_2D, NHD_2, H_2O_2, H_3O^+, CH_3OH, and CH_3NH_2 in their tunneling and tunneling-rotational modes are considered. It is shown that sensitivity coefficients strongly depend on the quantum numbers of the corresponding transitions. This can be used for astrophysical tests of Einstein's Equivalence Principle all over the Universe at an unprecedented level of sensitivity of $\sim 10^{-9}$, which is a limit three to two orders of magnitude lower as compared to the current constraints on cosmological variations of α and μ: $\Delta\alpha/\alpha < 10^{-6}$, $\Delta\mu/\mu < 10^{-7}$.

1 Introduction

The fundamental laws of particle physics, in our current understanding, depend on 28 constants including the gravitational constant, G, the mass, m_e, and charge, e, of the electron, the masses of six quarks, m_u, m_d, m_c, m_s, m_t, and m_b, the Planck constant, $\hbar$, the Sommerfeld constant α, the coupling constants of the weak, g_w, and strong, g_s, interactions, etc. The numerical values of these constants are not calculated within the Standard Model and remain, as Feynman wrote about the fine structure constant α in 1985, "one of the greatest mysteries of physics" [1]. However, it is natural to ask whether these constants are really constants, or whether they vary with the age of the universe, or over astronomical distances.

The idea that the fundamental constants may vary on the cosmological time scale has been discussing in different forms since 1937, when Milne and Dirac argued about possible variations of the Newton constant G during the lifetime of the universe [2, 3]. Over the past few decades, there have been extensive searches for persuasive evidences of the variation of physical constants. So far, there was found no one of them. The current limits for dimensionless constants such as the fine structure constant, $\alpha = e^2/\hbar c$, and the electron to proton mass ratio, $\mu = m_e/m_p$, obtained in laboratory experiments and from the Oklo natural reactor are on the order of one part in $10^{15} - 10^{17}$ [4–6] and one part in $10^{14} - 10^{16}$ [7–9] per year, respectively. The detailed discussion of ideas behind laboratory experiments can be found in a review [10].

Assuming that the constants are linearly dependent on the cosmic time, the same order of magnitude constraints on the fractional changes in $\Delta\alpha/\alpha = (\alpha_{obs} - \alpha_{lab})/\alpha_{lab}$ and in $\Delta\mu/\mu = (\mu_{obs} - \mu_{lab})/\mu_{lab}$ are stemming from astronomical observations of extragalactic objects at redshifts $z \sim 1 - 5$ [11–15]. Less stringent constraints at a percent level have been obtained from the cosmic microwave background (CMB) at $z \sim 10^3$ [16–18] and big bang nucleosynthesis (BBN) at $z \sim 10^{10}$

* Corresponding author E-mail: lev@astro.ioffe.rssi.ru
[1] Petersburg Nuclear Physics Institute, 188300 Gatchina
[2] St. Petersburg Electrotechnical University "LETI", Prof. Popov Str. 5, 197376 St. Petersburg
[3] Ioffe Physical-Technical Institute, Polytekhnicheskaya Str. 26, 194021 St. Petersburg

[19,20]. We note that space and/or time dependence of α based on optical spectra of quasars and discussed in the literature [21, and references therein] is still controversial and probably caused by systematic effects since independent radio-astronomical observations, which are more sensitive, show only null results for both $\Delta\alpha/\alpha$ and $\Delta\mu/\mu$ [22,23].

Surprisingly, it looks as if the Einstein heuristic principle of local position invariance (LPI) — *the outcome of any local non-gravitational experiment is independent of where and when in the universe it is performed* — is valid all over the universe, i.e., at the level of $\sim 10^{-6}$ neither α no μ deviate from their terrestrial values for the passed 10^{10} yr. In the Milky Way, it was also found no statistically significant deviations of $\Delta\mu/\mu$ from zero at even more deeper level of $\sim 10^{-8}$ [24–26].

However, the violation of the LPI was predicted in some theoretical models such as, for example, the theory of superstrings which considers time variations of α, g_w, and the QCD scale Λ_{QCD} (i.e., μ since $m_p \propto \Lambda_{QCD}$) and thereby opening a new window on physics beyond the Standard Model [27, and references therein]. If the fundamental constants are found to be changing in space and time, then they are not absolute but dynamical quantities which follow some deeper physical laws that have to be understood. Already present upper limits on the variation of the fundamental constants put very strong constraints on the theories beyond the Standard Model [28, and references therein]. This motivates the need for more precise laboratory and astronomical tests of the LPI. Of course, there are also other attempts to look for the new physics. For example the electric dipole moments (EDMs) of the elementary particles are very sensitive to the different extensions of the Standard Model. Present limit on the EDM of the electron significantly constrains supersymmetrical models and other theories [29,30].

In this review we will consider tests of LPI which are based on the analysis of microwave and submillimeter[1] astronomical spectra and which are essentially more sensitive to small variations in α and μ than the test based on optical spectral observations of quasars.

[1] The frequency range 1 GHz $\leq \nu \leq$ 300 GHz is usually referred to as a microwave range. Molecular transitions below 1 GHz (wavelength $\lambda > 30$ cm) are from a low-frequency range which is restricted by the ionospheric cut-off at 10 MHz ($\lambda = 30$ m).

2 Differential measurements of $\Delta\alpha/\alpha$ and $\Delta\mu/\mu$ from atomic and molecular spectra of cosmic objects

Speaking about stable matter, as, for example, atoms and molecules, we have only seven physical constants that describe their spectra [31]:

$$G,\ \Lambda_{QCD},\ \alpha,\ m_e,\ m_u,\ m_d,\ m_s.$$

The QCD scale parameter Λ_{QCD} and the masses of the light quarks u, d, and s contribute to the nucleon mass m_p (with $\Lambda_{QCD} \gg m_u + m_d + m_s$) and, thus, the electron-to-proton mass ratio μ is a physical constant characterizing the strength of electroweak interaction in terms of the strong interaction.

In the nonrelativistic limit and for an infinitely heavy pointlike nucleus all atomic transition frequencies are proportional to the Rydberg constant, R, and the ratios of atomic frequencies do not depend on any fundamental constants. Relativistic effects cause corrections to atomic energy, which can be expanded in powers of α^2 and $\alpha^2 Z^2$, the leading term being $\alpha^2 Z^2 R$, where Z is atomic number. Corrections accounting for the finite nuclear mass are proportional to $R\mu/Z$, but for atoms they are much smaller than relativistic corrections.

Astronomical differential measurements of the dimensionless constants α and μ are based on the comparison of the line centers in the absorption/emission spectra of cosmic objects and the corresponding laboratory values. It follows that the uncertainties of the laboratory rest frequencies and the line centers in astronomical spectra are the prime concern of such measurements. It is easy to estimate the natural bounds set by these uncertainties on the values of $\Delta\alpha/\alpha$ and $\Delta\mu/\mu$.

Consider the dependence of an atomic frequency ω on α in the comoving reference frame of a distant object located at redshift z [32,33]:

$$\omega_z = \omega + qx + O(x^2), \quad x \equiv (\alpha_z/\alpha)^2 - 1. \tag{1}$$

Here ω and ω_z are the frequencies corresponding to the present-day value of α and to a change $\alpha \to \alpha_z$ at a redshift z. In this relation, the so-called q factor is an individual parameter for each atomic transition.

If $\alpha_z \neq \alpha$, the quantity x in (1) differs from zero and the corresponding frequency shift $\Delta\omega = \omega_z - \omega$ is given by

$$\frac{\Delta\omega}{\omega} = Q\frac{\Delta\alpha}{\alpha}, \tag{2}$$

where $Q = 2q/\omega$ is the dimensionless sensitivity coefficient and $\Delta\alpha = (\alpha_z - \alpha)/\alpha$ is the fractional change in α. Here we assume that $|\Delta\alpha/\alpha| \ll 1$. The condition $\alpha_z \neq \alpha$ leads to a change in the apparent redshift of the distant object $\Delta z = \tilde{z} - z$:

$$\frac{\Delta\omega}{\omega} = -\frac{\Delta z}{1+z} \equiv \frac{\Delta v}{c}\,, \tag{3}$$

where Δv is the Doppler radial velocity shift.

If ω' is the observed frequency from the distant object, then the true redshift is given by

$$1 + z = \frac{\omega_z}{\omega'}\,, \tag{4}$$

whereas the shifted (apparent) value is

$$1 + \tilde{z} = \frac{\omega}{\omega'}\,. \tag{5}$$

Now, if we have two lines of the same element with the apparent redshifts $\tilde{z}_1$ and $\tilde{z}_2$ and the corresponding sensitivity coefficients Q_1 and Q_2, then

$$\Delta Q \frac{\Delta\alpha}{\alpha} = \frac{\tilde{z}_1 - \tilde{z}_2}{1+z} = \frac{\Delta v}{c}\,. \tag{6}$$

Here $\Delta v = v_1 - v_2$ is the difference of the measured radial velocities of these lines, and $\Delta Q = Q_2 - Q_1$ is the corresponding difference between their sensitivity coefficients. By comparing the apparent redshifts of two lines with different sensitivity coefficients Q we can study variation of α on a cosmological timescale.

Unfortunately, optical and UV transitions of atoms and molecules are not very sensitive to changes in α and μ. The sensitivity coefficients of atomic resonance transitions of usually observed in quasar spectra chemical elements (C, N, O, Na, Mg, Al, Si, S, Ca, Ti, Cr, Mn, Fe, Co, Ni, Zn) are very small, $Q \sim (\alpha Z)^2 \ll 1$ [34]. The same order of magnitude sensitivity coefficients to μ variations have been calculated for the UV transitions in the Lyman and Werner bands of molecular hydrogen H_2 [35–37], and for the UV transitions in the $4th$ positive band system $A^1\Pi - X^1\Sigma^+$ of carbon monoxide CO [38].

Small values of Q and ΔQ put tough constraints on optical methods to probe $\Delta\alpha/\alpha$ and $\Delta\mu/\mu$. Let us consider an example of Fe II lines arising from the ground state $3d^6(^5D)4s$. In quasar spectra we observe 7 resonance transitions ranging from 1608 Å to 2600 Å with both signs sensitivity coefficients: $Q_{\lambda 1608} = -0.0322$, $Q_{\lambda 1611} = +0.0502$, and $Q \simeq +0.08$ for transitions with $\lambda > 2000$ Å [39, note a factor of two difference in the definition of the coefficients Q with the present work]. This gives us the maximum value of $\Delta Q \simeq 0.11$ which is known with an error of ∼30%. From (6) it follows that a variance of $\Delta\alpha/\alpha \sim 10^{-5}$ would induce a velocity offset $\Delta v \simeq 0.3$ km s^{-1} between the 1608 Å line and any of the line with $\lambda > 2000$ Å. We may neglect uncertainties of the rest frame wavelengths since they are ∼0.02 km s^{-1} [40]. If both iron line centers are measured in quasar spectra with the same error σ_v, then the error of the offset Δv is $\sigma_{\Delta v} = \sqrt{2}\sigma_v$. The error $\sigma_{\Delta v}$ is a statistical estimate of the uncertainty of Δv, and, hence, it should be less than the absolute value of Δv. This gives us the following inequality to adjust parameters of spectral observations required to probe $\Delta\alpha/\alpha$ at a given level:

$$\sigma_v < \frac{\Delta Q}{\sqrt{2}} \frac{\Delta\alpha}{\alpha} c\,. \tag{7}$$

At $\Delta\alpha/\alpha \sim 10^{-5}$, the required position accuracy should be $\sigma_v \lesssim 0.25$ km s^{-1}. A typical error of the line center of an unsaturated absorption line in quasar spectra is about $1/10th$ of the pixel size (the wavelength interval between pixels) [41]. Current observations with the UV-Visual Echelle Spectrograph (UVES) at the ESO Very Large Telescope (VLT) provide a pixel size $\Delta\lambda_{\rm pix} \sim 0.05 - 0.06$ Å, i.e., at $\lambda \sim 5000$ Å the expected error σ_v should be ∼0.3 km s^{-1}, which is comparable to the velocity offset due to a fractional change in α at the level of 10^{-5}. Such a critical relationship between the 'signal' (expected velocity offset Δv) and the error σ_v hampers measuring $\Delta\alpha/\alpha$ at the level of $\sim 10^{-5}$ from any absorption system taking into account all imperfections of the spectrograph and the data reduction procedure. Systematic errors exceeding 0.5 km s^{-1} are known to be typical for the wavelength calibration in both the VLT/UVES and Keck/HIRES spectrographs [12,42–44]. At this level of the systematic errors an estimate of $\Delta\alpha/\alpha$ from any individual absorption-line system must be considered as an *upper limit* but not a 'signal'. Otherwise, a formal statistical analysis of such values may lead to unphysical results (examples can be found in the literature).

The UV molecular spectra of H_2 and CO observed at high redshifts in the optical wavelength band encounter with similar difficulties and restrictions. The maximum difference between the sensitivity coefficients in case of H_2 is $\Delta Q \sim 0.06$, the rest frame wavelength uncertainties are negligible, $\sim 5 \times 10^{-9}$ [45], and with the current spectral facilities at giant telescopes it is hard to get estimates of $\Delta\mu/\mu$ at a level deeper than 10^{-5}. For carbon monoxide such measurements have not been done so far but the expected limit on $\Delta\mu/\mu$ should be $\gtrsim 10^{-5}$ since CO lines are much weaker than H_2 [46] and therefore their line centers are less certain. The analogue of Eq. (6) for

the μ-estimation from a pair of molecular lines is [47]:

$$\frac{\Delta\mu}{\mu} = \frac{\Delta v}{c\Delta Q} = \frac{v_1 - v_2}{c(Q_2 - Q_1)}\,, \tag{8}$$

and for a given level of $\Delta\mu/\mu$, molecular line centers should be measured with an error

$$\sigma_v < \frac{\Delta Q}{\sqrt{2}}\frac{\Delta\mu}{\mu}c\,. \tag{9}$$

This means that at $\Delta\mu/\mu \sim 10^{-5}$, the required position accuracy should be $\sigma_v \lesssim 0.13$ km s^{-1}, or the pixel size $\Delta\lambda_{\rm pix} \lesssim 0.017$ Å at 4000 Å. This requirement was realized in the VLT/UVES observations of the quasar Q0347–383 [48] where a limit on $\Delta\mu/\mu$ of $(4.3 \pm 7.2) \times 10^{-6}$ was set.

At present the only way to probe variation of the fundamental constants on the cosmological timescale at a level deeper than 10^{-5} is to switch from optical to far infrared and microwave bands. In the microwave, or submillimeter range there are a good deal of molecular transitions arising in Galactic and extragalactic sources. Electronic, vibrational, and rotational energies in molecular spectra are scaled as $E_{\rm el} : E_{\rm vib} : E_{\rm rot} = 1 : \mu^{1/2} : \mu$. In other words, the sensitivity coefficients for pure vibrational and rotational transitions are equal to $Q_\mu = 0.5$ and $Q_\mu = 1$, respectively. Besides, molecules have fine and hyperfine structures, Λ-doubling, hindered rotation, accidental degeneracy between narrow close-lying levels of different types, which have a specific dependence on the physical constants. The advantage of radio observations is that some of these molecular transitions are approximately 100–1000 times more sensitive to variations of μ and/or α than optical and UV transitions.

In the far infrared waveband also lie atomic fine-structure transitions, which have sensitivity to α-variation $Q_\alpha \approx 2$ [49]. We can combine observations of these lines and rotational molecular transitions to probe a combination $F = \alpha^2/\mu$ [50]. Besides, radio-astronomical observations allow us to measure emission lines from molecular clouds in the Milky Way with an extremely high spectral resolution (channel width $\sim$0.02 km s^{-1}) leading to stringent constraints at the level of $\sim 10^{-9}$ [24]. The level 10^{-9} is a natural limit for radio-astronomical observations since it requires the rest frequencies of molecular transitions to be known with an accuracy better than 100 Hz. At the moment only ammonia inversion transitions and 18 cm OH Λ-doublet transitions have been measured in the laboratory with such a high accuracy [51, 52].

In the next sections we consider in more detail the sensitivities of different types of molecular transitions to changes in α and μ. We are mainly dealing with molecular lines observed in microwave and submillimeter ranges in the interstellar medium, but a few low-frequency transitions with high sensitivities are also included in our analysis just to extend the list of possible targets for future studies at the next generation of large telescopes for low-frequency radio astronomy.

3 Diatomic radicals in the Π ground state: CH, OH, and NH^+

We start our analysis of the microwave spectra of molecules from the simplest systems — diatomic molecules with nonzero projection of the electronic angular momentum $\boldsymbol{L}$ on the molecular axis. Several such molecules are observed in the interstellar medium. Here we will mostly focus on the two most abundant species — CH and OH. Recently it was realized that Λ-doublet transitions in these molecules have high sensitivity to the variation of both α and μ [53–55]. There are also several relatively low frequency transitions between rotational levels of the ground state doublet $\Pi_{1/2}$ and $\Pi_{3/2}$ with sensitivities, which are significantly different from the typical rotational ones [56]. Then we will briefly discuss the NH^+ radical[2], which is interesting because it has very low lying excited electronic state $^4\Sigma^-$. This leads to an additional enhancement of the dimensionless sensitivity coefficients Q [58]. The latter are defined as follows:

$$\frac{\Delta\omega}{\omega} = Q_\alpha\frac{\Delta\alpha}{\alpha} + Q_\mu\frac{\Delta\mu}{\mu}\,. \tag{10}$$

3.1 Λ-doubling and Ω-doubling

Consider electronic state with nonzero projection Λ of the orbital angular momentum on the molecular axis. The spin-orbit interaction couples electron spin $\boldsymbol{S}$ to the molecular axis, its projection being Σ. To a first approximation the spin-orbit interaction is reduced to the form $H_{so} = A\Lambda\Sigma$. Total electronic angular momentum $\boldsymbol{J}_e = \boldsymbol{L} + \boldsymbol{S}$ has projection Ω on the axis, $\Omega = \Lambda + \Sigma$. For a particular case of $\Lambda = 1$ and $S = \frac{1}{2}$ we have two states $\Pi_{1/2}$ and $\Pi_{3/2}$ and the energy difference between them is: $E(\Pi_{3/2}) - E(\Pi_{1/2}) = A$.

Rotational energy of the molecule is described by the Hamiltonian:

[2] NH^+ has not yet been detected in space, its fractional abundance in star-forming regions is estimated $N(NH^+)/N(H_2) \lesssim 4 \times 10^{-10}$ [57].

$$H_{\rm rot} = B(\boldsymbol{J} - \boldsymbol{J}_e)^2 \tag{11a}$$

$$= B\boldsymbol{J}^2 - 2B(\boldsymbol{J}\boldsymbol{J}_e) + B\boldsymbol{J}_e^2\,, \tag{11b}$$

where B is the rotational constant and $\boldsymbol{J}$ is the total angular momentum of the molecule. The first term in expression (11b) describes conventional rotational spectrum. The last term is constant for a given electronic state and can be added to the electronic energy.[3] The second term describes Ω-doubling and is known as the Coriolis interaction $H_{\rm Cor}$.

If we neglect the Coriolis interaction, the eigenvectors of Hamiltonian (11) have definite projections M and Ω of the molecular angular momentum $\boldsymbol{J}$ on the laboratory axis and on the molecular axis respectively. In this approximation the states $|J, M, \Lambda, \Sigma, \Omega\rangle$ and $|J, M, -\Lambda, -\Sigma, -\Omega\rangle$ are degenerate, $E_{J,\pm\Omega} = BJ(J+1)$. The Coriolis interaction couples these states and removes degeneracy. New eigenstates are the states of definite parity $p = \pm 1$ [59]:

$$|J, M, \Omega, p\rangle = (|J, M, \Omega\rangle + p(-1)^{J-S}|J, M, -\Omega\rangle)/\sqrt{2}. \tag{12}$$

The operator $H_{\rm Cor}$ can only change quantum number Ω by one, so the coupling of states $|\Omega\rangle$ and $|-\Omega\rangle$ takes place in the 2Ω order of the perturbation theory in $H_{\rm Cor}$.

The Ω-doubling for the state $\Pi_{1/2}$ happens already in the first order in the Coriolis interaction, but has additional smallness from the spin-orbit mixing. The operator $H_{\rm Cor}$ can not directly mix degenerate $|\Lambda, \Sigma, \Omega\rangle$ states $|1, -\frac{1}{2}, \frac{1}{2}\rangle$ and $|-1, \frac{1}{2}, -\frac{1}{2}\rangle$ because it requires changing Λ by two. Therefore, we need to consider spin-orbit mixing of the Π and Σ states:

$$\left|\Omega = \frac{1}{2}\right\rangle = \left|1, -\frac{1}{2}, \frac{1}{2}\right\rangle + \zeta \left|0, \frac{1}{2}, \frac{1}{2}\right\rangle, \tag{13}$$

where

$$\zeta \sim A/(E_\Pi - E_\Sigma), \tag{14}$$

and then

$$\left\langle \Omega = \frac{1}{2}\middle| H_{\rm Cor} \middle|\Omega = -\frac{1}{2}\right\rangle = 2\zeta B\left(J + \frac{1}{2}\right)\langle \Lambda = 1|L_x|\Lambda = 0\rangle. \tag{15}$$

[3] Note that this term contributes to the separation between the states $\Pi_{1/2}$ and $\Pi_{3/2}$. This becomes particularly important for light molecules, where the constant A is small.

Note that ζ depends on the non-diagonal matrix element (ME) of the spin-orbit interaction and Eq. (14) is only an order of magnitude estimate. It is important, though, that non-diagonal and diagonal MEs have similar dependence on fundamental constants. We conclude that Ω-splitting for the $\Pi_{1/2}$ level must scale as $ABJ/(E_\Pi - E_\Sigma)$. The Ω-doubling for $\Pi_{3/2}$ state takes place in the third order in the Coriolis interaction. Here $H_{\rm Cor}$ has to mix first states $\Pi_{3/2}$ with $\Pi_{1/2}$ and $\Pi_{-3/2}$ with $\Pi_{-1/2}$ before ME (15) can be used. Therefore, the splitting scales as $B^3J^3/[A(E_\Pi - E_\Sigma)]$.

The above consideration corresponds to the coupling case *a*, when $|A| \gg B$. In the opposite limit the states $\Pi_{1/2}$ and $\Pi_{3/2}$ are strongly mixed by the Coriolis interaction and spin $\boldsymbol{S}$ decouples from the molecular axis (coupling case *b*). As a result, the quantum numbers Σ and Ω are not defined and we only have one quantum number $\Lambda = \pm 1$. The Λ-splitting takes place now in the second order in the Coriolis interaction via intermediate Σ states. The scaling here is obviously of the form $B^2J^2/(E_\Pi - E_\Sigma)$. Note that in contrast to the previous case $|A| \gg B$, the splitting here is independent on A.

We can now use found scalings of the Λ- and Ω-doublings to determine sensitivity coefficients (10). We only need to recall that in atomic units $A \propto \alpha^2$ and $B \propto \mu$. We conclude that for the case *a* the Ω-doubling spectrum has following sensitivity coefficients:

$$\text{State } {}^2\Pi_{1/2}: \quad Q_\alpha = 2\,, \quad Q_\mu = 1\,, \tag{16a}$$

$$\text{State } {}^2\Pi_{3/2}: \quad Q_\alpha = -2\,, \quad Q_\mu = 3\,. \tag{16b}$$

For the case *b*, when $\boldsymbol{S}$ is completely decoupled from the axis, the Λ-doubling spectrum has following sensitivity coefficients:

$$\text{State } \Pi: \quad Q_\alpha = 0\,, \quad Q_\mu = 2\,. \tag{16c}$$

When constant A is slightly larger than B, the spin $\boldsymbol{S}$ is coupled to the axis only for lower rotational levels. As rotational energy grows with J and becomes larger than the splitting between states $\Pi_{1/2}$ and $\Pi_{3/2}$, the spin decouples from the axis. Consequently, the Ω-doubling is transformed into Λ-doubling. Equations (16) show that this can cause significant changes in sensitivity coefficients. The spin-orbit constant A can be either positive (CH molecule), or negative (OH). The sign of the Ω-doubling depends on the sign of A, while Λ-doubling does not depend on A at all. Therefore, decoupling of the spin can change the sign of the splitting. In Sec. 3.2 we will see that this can lead to a dramatic enhancement of the sensitivity to the variation of fundamental constants.

3.2 Intermediate coupling

The Λ-doubling for the intermediate coupling was studied in detail in many papers, including [63–65] (see also the book [59]). Here we use the effective Hamiltonian $H_{\rm eff}$ from [63] in the subspace of the levels $\Pi^{\pm}_{1/2}$ and $\Pi^{\pm}_{3/2}$, where upper sign corresponds to the parity p in Eq. (12). The operator $H_{\rm eff}$ includes spin-rotational and hyperfine parts

$$H_{\rm eff} = H_{\rm sr} + H_{\rm hf}\,. \tag{17}$$

Neglecting third order terms in the Coriolis and spin-orbit interactions, we get the following simplified form of the spin-rotational part:

$$\langle \Pi_{1/2},\, J,\, p|\, H_{\rm sr}|\Pi_{1/2},\, J,\, p\rangle = -\frac{1}{2}A + B\left(J+\frac{1}{2}\right)^2 + p(S_1+S_2)(2J+1)\,, \tag{18a}$$

$$\langle \Pi_{3/2},\, J,\, p|\, H_{\rm sr}|\Pi_{3/2},\, J,\, p\rangle = +\frac{1}{2}A + B\left(J+\frac{1}{2}\right)^2 - 2B\,, \tag{18b}$$

$$\langle \Pi_{3/2},\, J,\, p|\, H_{\rm sr}|\Pi_{1/2},\, J,\, p\rangle = \left[B + pS_2\left(J+\frac{1}{2}\right)\right] \times\sqrt{\left(J-\frac{1}{2}\right)\left(J+\frac{3}{2}\right)}\,. \tag{18c}$$

Here in addition to the parameters A and B we have two parameters which appear in the second order of perturbation theory via intermediate state(s) $\Sigma_{1/2}$. The parameter S_1 corresponds to the cross term of the perturbation theory in the spin-orbit and Coriolis interactions, while the parameter S_2 is quadratic in the Coriolis interaction. Because of this S_1 scales as $\alpha^2\mu$ and S_2 scales as μ^2. It is easy to see that the Hamiltonian $H_{\rm sr}$ describes limiting cases $|A| \gg B$ and $|A| \ll B$ considered in Sec. 3.1.

The hyperfine part of the effective Hamiltonian is defined in the lowest order of perturbation theory and has the form:

$$\langle \Pi_{1/2},\, J,\, p|\, H_{\rm hf}|\Pi_{1/2},\, J,\, p\rangle = C_F[2a - b - c + p(2J+1)d], \tag{19a}$$

$$\langle \Pi_{3/2},\, J,\, p|\, H_{\rm hf}|\Pi_{3/2},\, J,\, p\rangle = 3C_F\,[2a + b + c]\,, \tag{19b}$$

$$\langle \Pi_{3/2},\, J,\, p|\, H_{\rm hf}|\Pi_{1/2},\, J,\, p\rangle = -C_F\sqrt{(2J-1)(2J+3)}\,b, \tag{19c}$$

$$C_F \equiv [F(F+1) - J(J+1) - I(I+1)][8J(J+1)]^{-1}\,.$$

Here we assume that only one nucleus has spin and include only magnetic dipole hyperfine interaction.

The effective Hamiltonian described by Eqs. (18, 19) has 8 parameters. We use NIST values [60] for the fine structure splitting A, rotational constant B, and magnetic hyperfine constants a, b, c, d. Remaining two parameters S_1 and S_2 are found by minimizing the *rms* deviation between theoretical and experimental Λ-doubling spectra.

In order to find sensitivity coefficients Q_α we calculate transition frequencies for two values of $\alpha = \alpha_0 \pm \delta$ near its physical value $\alpha_0 = 1/137.035999679(94)$. The similar procedure is applied to Q_μ at the physical value of the electron-to-proton mass ratio, $\mu_0 = 1/1836.15267247(80)$. We use scaling rules discussed above to recalculate parameters of the effective Hamiltonian for different values of fundamental constants. Then we use numerical differentiation to find respective sensitivity coefficient.

3.3 Sensitivity coefficients for Λ-doublet transitions in CH and OH

In Ref. [55], the method described in the previous section was applied to ^{16}OH, ^{12}CH, ^{7}Li^{16}O, ^{14}N^{16}O, and ^{15}N^{16}O. The molecules CH and NO have ground state $^2\Pi_{1/2}$ ($A > 0$), while OH and LiO have ground state $^2\Pi_{3/2}$ ($A < 0$). The ratio $|A/B|$ changes from 2 for CH molecule [66], to 7 for OH [67], and to almost a hundred for LiO and NO. Therefore, LiO and NO definitely belong to the coupling case *a*. For OH molecule we can expect transition from case *a* for lower rotational states to case *b* for higher ones. Finally, for CH we expect intermediate coupling for lower rotational states and coupling case *b* for higher states.

Let us see how this scheme works in practice for the effective Hamiltonian (18, 19). Figure 1 demonstrates J-dependence of the sensitivity coefficients for CH and OH molecules. Both of them have only one nuclear spin $I = \frac{1}{2}$. For a given quantum number J, each Λ-doublet transition has four hyperfine components: two strong transitions with $\Delta F = 0$ and $F = J \pm \frac{1}{2}$ (for $J = \frac{1}{2}$ there is only one transition with $F = 1$) and two weaker transitions with $\Delta F = \pm 1$. The hyperfine structure for OH and CH molecules is rather small and sensitivity coefficients for all hyperfine components are very close. Because of

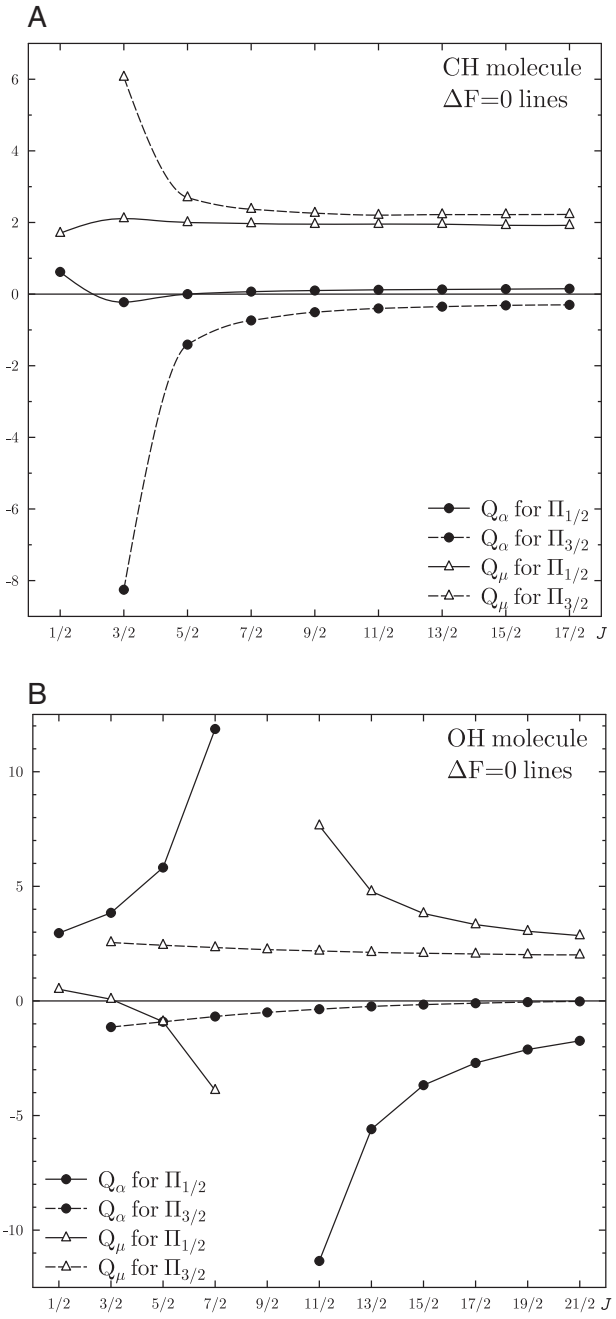

Figure 1 Sensitivity coefficients Q_α and Q_μ for Λ-doublet lines with $\Delta F = 0$ in CH and OH. The difference between lines with $F = J + \frac{1}{2}$ and $F = J - \frac{1}{2}$ is too small to be seen. For the state $\Pi_{3/2}$ of OH the values for $J = \frac{9}{2}$ are too large to be shown on the plot. They are listed in Table 1.

that Fig. 1 presents only averaged values for strong transitions with $\Delta F = 0$.

We see that for large values of J the sensitivity coefficients for both molecules approach limit (16c) of the coupling case *b*. The opposite limits (16a, 16b) are not reached for either molecule even for smallest values of J. So, we conclude that the coupling case *a* is not realized. It is interesting that in Fig. 1 the curves for the lower states are smooth, while for upper states there are singularities. For CH molecule this singularity takes place for the state $\Pi_{3/2}$ near the lowest possible value $J = 3/2$. A singularity for OH molecule takes place for the state $\Pi_{1/2}$ near $J = 9/2$.

These singularities appear because Λ-splitting turns to zero. As we saw above, the sign of the splitting for the coupling case *a* depends on the sign of the constant A. The same sign determines which state $\Pi_{1/2}$, or $\Pi_{3/2}$ lies higher. As a result, for the lower state the sign of the splitting is the same for both limiting cases, but decoupling of the electron spin S for the upper state leads to the change of sign of the splitting. Of course, these singularities are most interesting for our purposes, as they lead to large sensitivity coefficients which strongly depend on the quantum numbers. Note, that when the frequency of the transition is small, it becomes sensitive to the hyperfine part of the Hamiltonian and the sensitivity coefficients for hyperfine components may differ significantly. The sensitivity coefficients of all hyperfine components of such Λ-lines are given in Table 1. We can see that near the singularities all sensitivity coefficients are enhanced.

In addition to Λ-doublet transitions and purely rotational transitions there are also mixed transitions between rotational states of $\Pi_{1/2}$ and $\Pi_{3/2}$ states. The transition energy here includes the rotational and the fine structure parts. Because of that, such transitions may have different sensitivities to the variation of fundamental constants [56]. As an example, Fig. 2 shows mixed transitions in CH molecule. The sensitivity coefficients are given in Table 2. The isotopologue CD has mixed transitions of lower frequencies and higher sensitivities [56]. Similar picture takes place for OH molecule.

The molecule NH^+ is isoelectronic to CH and also has ground state $^2\Pi_{1/2}$. However, there is an important difference: for NH^+ the first excited state $^4\Sigma^-$ lies only 340 cm^{-1} above the ground state [68, 69]. The spin-orbit interaction between these states leads to strong perturbations of the rotational structure and of the Λ-doublet splittings and to an additional enhancement of the sensitivity coefficients [58]. The spectrum of NH^+ is shown in Fig. 3. The effective Hamiltonian is similar to the one considered above with two additional terms describing interaction between the $^2\Pi$ and $^4\Sigma$ states [68]:

$$\langle {}^2\Pi_{3/2},\, J,\, p|\, H_{\rm so}|{}^4\Sigma^-_{3/2},\, J,\, p\rangle = -\frac{1}{2}\zeta_{3/2}\,, \tag{20a}$$

$$\langle {}^2\Pi_{1/2},\, J,\, p|\, H_{\rm so}|{}^4\Sigma^-_{1/2},\, J,\, p\rangle = -\frac{1}{2\sqrt{3}}\zeta_{1/2}\,. \tag{20b}$$

Table 1 Frequencies (in MHz) and sensitivity coefficients for hyperfine components $(J, F \to J, F')$ of Λ-doublet lines in CH and OH molecules. Recommended frequencies and their uncertainties are taken from [60–62].

					ω (MHz)					
Molecule	Level	J	F	F'	Recom.	Uncert.	Theory	Diff.	Q_α	Q_μ
^{12}CH	$^2\Pi_{1/2}$	0.5	0	1	3263.795	0.003	3269.40	− 5.61	0.59	1.71
		0.5	1	1	3335.481	0.001	3340.77	− 5.29	0.62	1.70
		0.5	1	0	3349.194	0.003	3354.11	− 4.92	0.63	1.69
		1.5	1	2	7275.004	0.001	7262.25	12.75	− 0.24	2.12
		1.5	1	1	7325.203	0.001	7312.02	13.18	− 0.23	2.11
		1.5	2	2	7348.419	0.001	7335.30	13.12	− 0.22	2.11
		1.5	2	1	7398.618	0.001	7385.08	13.54	− 0.20	2.10
^{12}CH	$^2\Pi_{3/2}$	1.5	2	2	701.68	0.01	682.96	18.72	− 8.44	6.15
		1.5	1	2	703.97	0.03	679.83	24.14	− 8.66	6.32
		1.5	2	1	722.30	0.03	702.98	19.52	− 8.37	6.17
		1.5	1	1	724.79	0.01	699.85	24.94	− 8.07	5.97
^{16}OH	$^2\Pi_{3/2}$	1.5	1	2	1612.2310	0.0002	1595.42	16.81	− 1.27	2.61
		1.5	1	1	1665.4018	0.0002	1648.93	16.47	− 1.14	2.55
		1.5	2	2	1667.3590	0.0002	1650.66	16.70	− 1.14	2.55
		1.5	2	1	1720.5300	0.0002	1704.17	16.36	− 1.02	2.49
^{16}OH	$^2\Pi_{1/2}$	0.5	0	1	4660.2420	0.0030	4638.98	21.26	2.98	0.50
		0.5	1	1	4750.6560	0.0030	4729.51	21.15	2.96	0.51
		0.5	1	0	4765.5620	0.0030	4744.50	21.06	2.96	0.51
		4.5	5	4	88.9504	0.0011	64.34	24.61	− 921.58	459.86
		4.5	5	5	117.1495	0.0011	92.35	24.80	− 699.65	349.59
		4.5	4	4	164.7960	0.0011	141.20	23.60	− 496.67	248.77
		4.5	4	5	192.9957	0.0011	169.22	23.78	− 424.05	212.68

Obviously, the parameters $\zeta_{1/2}$ and $\zeta_{3/2}$ scale as α^2. As mentioned above, for the NH^+ molecule the splitting between Σ and Π states $\Delta E_{\Sigma\Pi}$ is only about 340 cm^{-1}. This splitting includes three contributions: the non-relativistic electronic energy difference, the relativistic corrections ($\sim\alpha^2 Z^2$) and the difference in the zero point vibrational energies for the two states ($\sim\mu^{1/2}$). Note that the accidental degeneracy of these levels for NH^+ means that the first contribution is anomalously small. Because of that, the other two contributions can not be neglected and modify the scaling of $\Delta E_{\Sigma\Pi}$ with fundamental constants. This effect has to be taken into account in the calculations of the sensitivity coefficients [58].

4 Linear polyatomic radicals in the Π ground state: C_3H

The linear form of the molecule C_3H (l-C_3H) is similar to the molecule NH^+: it also has the ground state $^2\Pi_{1/2}$ and two closely lying states $^2\Pi_{3/2}$ and $^2\Sigma^+_{1/2}$. Here the quasi

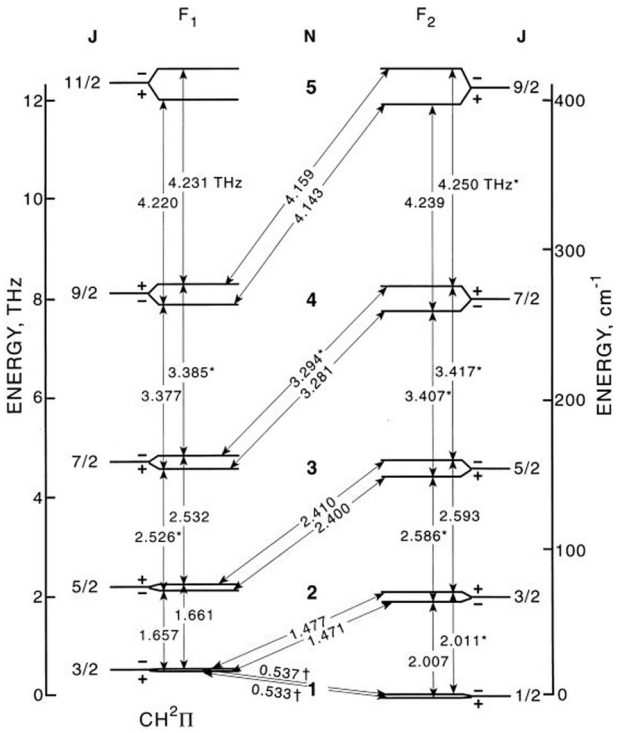

Figure 2 Rotational spectrum of CH from [66]. Vertical and diagonal arrows correspond to pure rotational and mixed transitions, respectively. Λ-doubling is not to scale.

Table 2 Frequencies (GHz) and sensitivities of the rotational and mixed transitions in CH.

N, J, p	N', J', p'	$\nu_{\rm theor}$	$\nu_{\rm expt}$ [62]	Q_α	Q_μ
$1, \frac{3}{2}, +$	$1, \frac{1}{2}, -$	533.9	532.7	1.59	0.20
$1, \frac{3}{2}, -$	$1, \frac{1}{2}, +$	537.9	536.8	1.57	0.22
$2, \frac{3}{2}, +$	$1, \frac{3}{2}, -$	1477.2	1477.4	0.00	1.00
$2, \frac{3}{2}, -$	$1, \frac{3}{2}, +$	1470.6	1470.7	−0.01	1.00
$2, \frac{5}{2}, +$	$1, \frac{3}{2}, -$	1663.0	1661.1	0.00	1.00
$2, \frac{5}{2}, -$	$1, \frac{3}{2}, +$	1658.8	1657.0	0.00	1.00
$2, \frac{3}{2}, +$	$1, \frac{1}{2}, -$	2011.8	2010.8	0.42	0.79
$2, \frac{3}{2}, -$	$1, \frac{1}{2}, +$	2007.8	2006.8	0.42	0.79
$2, \frac{5}{2}, +$	$2, \frac{3}{2}, -$	193.1	191.1	0.01	1.03
$2, \frac{5}{2}, -$	$2, \frac{3}{2}, +$	180.9	178.9	0.06	0.94

degeneracy of the Π and Σ states is not accidental, but is caused by the Renner-Teller interaction. In the following section we briefly recall the theory of the Renner-Teller effect in polyatomic linear molecules [70, 71].

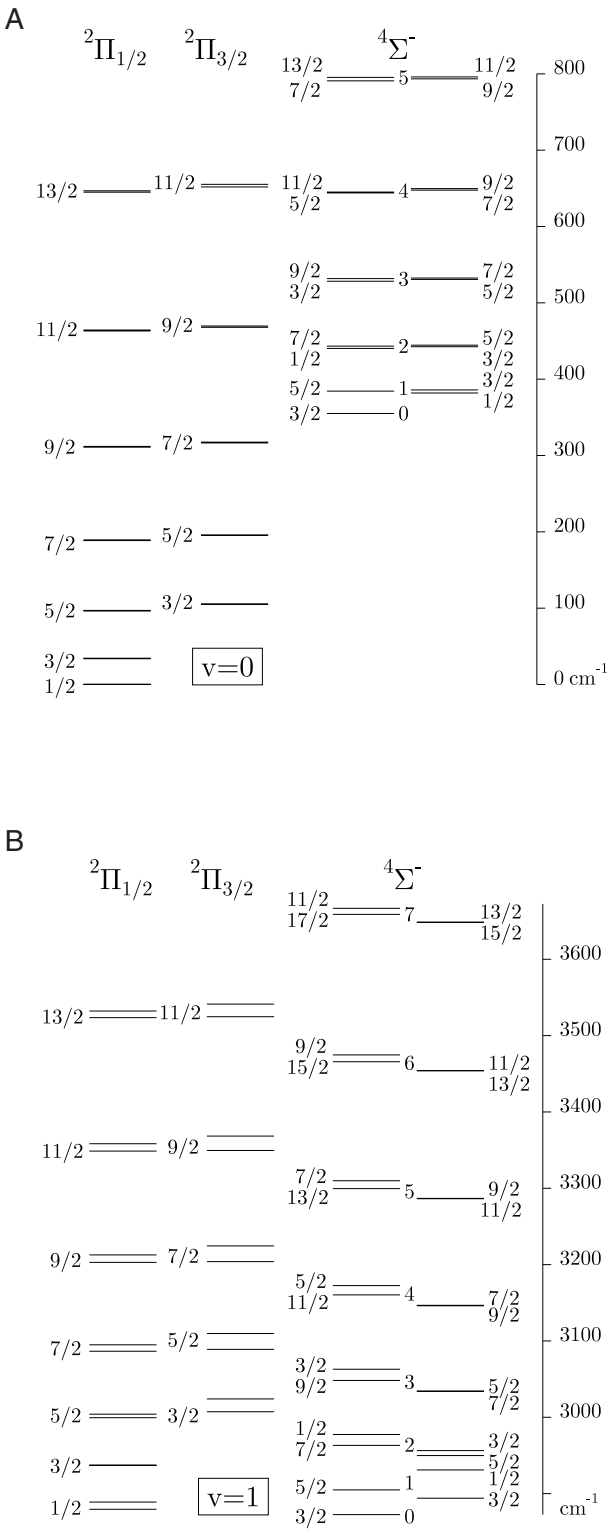

Figure 3 Spin-rotational levels of the three lowest electronic states of the molecule NH^+. Panels (A) and (B) correspond to vibrational states $v = 0$ and $v = 1$ respectively. The energy levels are labeled with the quantum number J for the Π states and with J and N for the Σ state.

4.1 Renner-Teller effect

The total molecular angular momentum of the polyatomic molecule $\boldsymbol{J}$ includes the vibrational angular momentum $\boldsymbol{G}$ associated with the twofold degenerate bending vibration mode(s): $\boldsymbol{J} = \boldsymbol{N} + \boldsymbol{S} = \boldsymbol{R} + \boldsymbol{G} + \boldsymbol{L} + \boldsymbol{S}$, where $\boldsymbol{R}$ describes rotation of the molecule as a whole and is perpendicular to the molecular axis ζ. Other momenta have nonzero ζ-projections: $\langle G_\zeta \rangle = l$, $\langle L_\zeta \rangle = \Lambda$, $\langle N_\zeta \rangle = K = l + \Lambda$, and $\langle J_\zeta \rangle = \Omega$.

Suppose we have Π electronic state $|\Lambda = \pm 1\rangle$ and $v = 1$ vibrational state of a bending mode $|l = \pm 1\rangle$. All together there are 4 states $|\Lambda = \pm 1\rangle|l = \pm 1\rangle$. We can rewrite them as one doublet Δ state $|K = \pm 2\rangle$ and states Σ^+ and Σ^-. In the adiabatic approximation all four states are degenerate. Renner [70] showed that the states with the same quantum number $K = l + \Lambda$ strongly interact, so the Σ^+ and Σ^- states repel each other, while the Δ doublet in the first approximation remains unperturbed. We are particularly interested in the case when one of the Σ levels is pushed close to the ground state $v = 0$. This is what takes place in the l-C_3H molecule [74–76].

Consider a linear polyatomic molecule with the unpaired electron in the π_ξ state in the molecular frame ξ, η, ζ. Obviously, the bending energy is different for bendings in $\xi\zeta$ and in $\eta\zeta$ planes: $V_\pm = \frac{1}{2} k_\pm \chi^2$ (here χ is the supplement to the bond angle). That means that the electronic energy depends on the angle ϕ between the electron and nuclear planes:

$$H' = V' \cos 2\phi \,, \tag{21}$$

where $2V' = V_+ - V_- = k'\chi^2$. There is no reason for V' to be small, so $k' \sim k_\pm \sim 1$ a.u. and to a first approximation k' does not depend on α and μ.

As long as interaction (21) depends on the relative angle between the electron and the vibrational planes, it changes the angular quantum numbers as follows: $\Delta\Lambda = -\Delta l = \pm 2$ and $\Delta K = 0$. This is exactly what is required to produce splitting between the Σ^+ and Σ^- states with $v = 1$ as discussed above.

Interaction (21) also mixes different vibrational levels with $\Delta v = \pm 2, \pm 4, \ldots$. Thus, we have, for example, the nonzero ME $\langle 0, 0, 1, 1|H'|2, 2, -1, 1\rangle$ between states $|v, l, \Lambda, K\rangle$. Such mixings reduce effective value of the quantum number Λ and, therefore, reduce the spin-orbital splitting between the $\Pi_{1/2}$ and $\Pi_{3/2}$ states [73],

$$H_{\rm so} \equiv A_{\rm eff} \Lambda \Sigma \,, \quad A_{\rm eff} = A\Lambda_{\rm eff}/\Lambda \,. \tag{22}$$

Let us define the model more accurately. Following [73] we write the Hamiltonian as:

$$H = H_e + T_v + A L_\zeta S_\zeta \,. \tag{23}$$

Here the "electronic" part H_e includes all degrees of freedom except for the bending vibrational mode and spin. For l-C_3H there are two bending modes, but for simplicity we include the second bending mode in H_e too. Electronic MEs in the $|\Lambda\rangle$ basis have the form:

$$\langle \pm 1|H_e|\pm 1\rangle = \frac{V_+ + V_-}{2} = \frac{k}{2}\chi^2 \,, \tag{24a}$$

$$\langle \pm 1|H_e|\mp 1\rangle = \frac{k'}{2}\chi^2 \exp(\mp 2i\phi) \,. \tag{24b}$$

Here χ and ϕ are the vibrational coordinates for the bending mode. Kinetic energy in these coordinates has the form:

$$T_v = -\frac{1}{2MR^2}\left(\frac{\partial^2}{\partial\chi^2} + \frac{1}{\chi}\frac{\partial}{\partial\chi} + \frac{1}{\chi^2}\frac{\partial^2}{\partial\phi^2}\right) . \tag{25}$$

We can use the basis set of 2D harmonic functions in polar coordinates $\rho = \chi R$ and ϕ for the mass M and the force constant k:

$$\psi_{v,l}(\rho, \phi) = R_{v,l}(\rho)\frac{1}{\sqrt{2\pi}} \exp(il\phi) \,. \tag{26}$$

It is important that the radial functions are orthogonal only for the same l:

$$\langle R_{v',l}|R_{v,l}\rangle = \delta_{v',v} \,. \tag{27}$$

This allows for the nonzero MEs between states with different quantum number l. By averaging operator (23) over vibrational functions we get:

$$\langle v', l'|H_e + T_v|v, l\rangle = \left[\omega_v(v+1) + A\Lambda S_\zeta\right]\delta_{v',v}\delta_{l',l} + \frac{1}{2}\langle R_{v'l'}|k'\chi^2|R_{vl}\rangle \exp(\mp 2i\phi)\delta_{l',l\pm 2} . \tag{28}$$

The exponent here ensures the selection rule $\Lambda' = \Lambda \mp 2$ for the quantum number Λ when we calculate MEs for the rotating molecule.

4.2 Molecule l-C_3H

We solve the eigenvalue problem for Hamiltonian (23) using the basis set of the 2D-harmonic oscillator. Our model Hamiltonian has only 3 parameters, namely ω_v, A, and the dimensionless Renner-Teller parameter $\mathcal{E}$:

Table 3 Low lying energy levels for the bending mode $\omega_\nu = 589$ cm^{-1} of l-C_3H molecule and their sensitivities q_α and q_μ to the variation of α and μ respectively. Δ is the distance from the ground state. All values are in cm^{-1}.

						Δ			
$\nu_{\rm nom}$	$\langle\nu\rangle$	K	Ω	$\langle\Lambda\rangle$	E	[72]	[73]	q_μ	q_α
0	1.22	1	0.5	0.50	367.9	0.0	0.0	187.8	−14.6
0	1.35	1	1.5	0.46	381.9	13.9	14.0	187.8	13.3
1	2.32	0	0.5	−0.01	394.2	26.3	27.0	197.3	−0.4
1	3.57	2	1.5	0.21	597.7	229.7	226.0	300.3	−6.1
1	3.65	2	2.5	0.19	603.5	235.5	232.0	300.3	5.5

Table 4 l-C_3H sensitivity coefficients for the transitions between states from Table 3 and for parameters $A_{\rm eff}$ and $\Delta E_{\Sigma\Pi}$ defined by (22) and (29) respectively. Frequencies are in cm^{-1}.

				Fit to [73]			Fit to [76]		
K	Ω	K'	Ω'	ω	Q_μ	Q_α	ω	Q_μ	Q_α
1	0.5	1	1.5	13.9	0.00	2.00	14.4	0.00	2.00
1	1.5	0	0.5	12.4	0.78	−1.11	13.3	0.77	−1.07
0	0.5	2	1.5	203.5	0.51	−0.03	204.4	0.51	−0.03
2	1.5	2	2.5	5.8	0.00	2.00	6.0	0.00	2.00
	$A_{\rm eff}$			13.9	0.00	2.00	14.4	0.00	2.00
	$\Delta E_{\Sigma\Pi}$			19.4	0.50	0.00	20.5	0.50	0.00

$k' = \mathcal{E}k$. The values for ω_ν and A for l-C_3H are given in [73]. We varied the Renner-Teller parameter $\mathcal{E}$ to fit five lowest levels for the given bending mode: $\Pi_{1/2}$, $\Pi_{3/2}$, $\Sigma_{1/2}$, $\Delta_{3/2}$, and $\Delta_{5/2}$. The optimal value appeared to be $\mathcal{E} = 0.788$. The results are presented in Table 3. The first two columns give nominal vibrational quantum number ν and its actual average value. We see that the Renner-Teller term in (28) strongly mixes vibrational states. This mixing also affects $\langle\Lambda\rangle$ and decreases spin-orbital splittings as explained by Eq. (22).

The last two columns in Table 3 give dimensional sensitivity coefficients q_μ and q_α in cm^{-1}:

$$\Delta E = q_\alpha \frac{\Delta\alpha}{\alpha} + q_\mu \frac{\Delta\mu}{\mu}\,.$$

To estimate them we assumed that the parameters scale in a following way: $\omega_\nu \sim \mu^{1/2}$, $A \sim \alpha^2$, and $\mathcal{E}$ does not depend on α and μ. The dimensionless sensitivity coefficients (10) for the transitions $\omega_{i,k} = E_k - E_i$ can be found as:

$$Q_{i,k} = (q_k - q_i)/\omega_{i,k}\,.$$

In Table 4 these coefficients are calculated for the same set of parameters as in Table 3 and for the slightly different parameters which better fit experimental frequencies from [76]. We see that the sensitivity coefficients are practically the same for both sets.

For the two fine structure transitions, $\Pi_{1/2} \longrightarrow \Pi_{3/2}$ and $\Delta_{3/2} \longrightarrow \Delta_{5/2}$, we get sensitivities $Q_\mu = 0$ and $Q_\alpha = 2$. This may seem strange as the fine structure is significantly reduced by the Renner-Teller mixing: the fine-structure parameter is 29 cm^{-1} and the splitting between $\Pi_{1/2}$ and $\Pi_{3/2}$ is only 13.9 cm^{-1}. According to (22) the mixing reduces the splitting. However, this effect depends on the dimensionless Renner-Teller parameter $\mathcal{E}$ and does not depend on μ and α. Consequently, *the effective parameter $A_{\rm eff}$ depends on fundamental constants in the same way as initial parameter A.*

For the high frequency transition $\Sigma_{1/2} \longrightarrow \Delta_{3/2}$, where the spin-orbital energy can be neglected, we get $Q_\mu = 0.5$ and $Q_\alpha = 0$. These results are expected, because our model has only two dimensional parameters: vibrational frequency, which is proportional to $\mu^{1/2}$ and the fine structure parameter A, which scales as α^2. Even though our vibrational spectrum is far from that of a simple harmonic oscillator, the non-diagonal MEs (28) of the Hamiltonian (23) still scale as $\mu^{1/2}$. Therefore, if we neglect spin-orbital splittings, we get $Q_\mu = 1/2$ for all transitions. The only transition in Table 4 where the spin-orbital energy and vibrational energy are close to each other is the $\Pi_{3/2} \longrightarrow \Sigma_{1/2}$ transition. The resultant frequency is roughly half of the vibrational energy difference between the Π and Σ states. This leads to $Q_\mu \approx 1$ and $Q_\alpha \approx -1$.

The spectrum of the l-C_3H molecule is shown on Fig. 4. The effective Hamiltonian for the rotating molecule is similar to that of the NH^+ molecule. It includes the effective fine-structure parameter $A_{\rm eff}$ and the energy difference between the Σ and Π states,

$$\Delta E_{\Sigma\Pi} = E(\Sigma^+) - \frac{E(\Pi_{1/2}) + E(\Pi_{3/2})}{2}\,. \qquad (29)$$

Numerical values for these parameter are obtained from the fit to the experimental transition frequencies. Here we only need to determine the dependence of these parameters on fundamental constants. Table 4 shows that $A_{\rm eff} \sim \alpha^2$ and $\Delta E_{\Sigma\Pi} \sim \mu^{1/2}$. Once again, this is because

the Renner-Teller mixing depends on the dimensionless parameter $\mathcal{E}$ and *does not* depend on α and μ. Calculated sensitivity coefficients for the K-doublet transitions of the l-C_3H molecule are listed in Tables 5 and 6. The results for the mixed transitions can be found in [72].

5 Tunneling modes in polyatomic molecules

In this section we consider non linear and non planar polyatomic molecules. Such molecules generally have more than one equivalent potential minimum. If the barriers between these minima are not too high the molecule can tunnel between them. Ammonia (NH_3) is the best known textbook example of a nonrigid molecule (see Fig. 5). Interestingly, this molecule is also one of the most abundoned polyatomic molecules in the interstellar medium. Other important for astrophysics molecules with tunneling include hydronium (H_3O^+), peroxide (H_2O_2), methanol (CH_3OH), and methylamine (CH_3NH_2). We will briefly discuss all of them below. All these molecules include only light atoms with $Z \leq 8$ and have singlet electronic ground states. Thus we can neglect relativistic corrections and assume that all discussed transitions have $Q_\alpha = 0$.

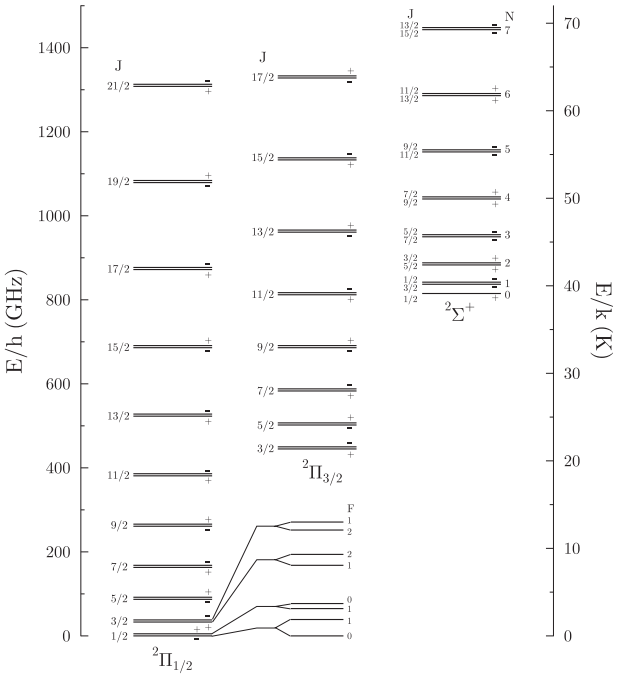

Figure 4 Spin-rotational levels of the three lowest vibronic states of the molecule l-C_3H. K-doubling is indicated schematically, hyperfine structure is shown only for the two lowest K-doublets. Due to a strong Renner-Teller effect the component $^2\Sigma^+$ of the excited bending state ν_4(CCH bending) is shifted towards lower energies, $\sim$29 cm^{-1} above the zero-level of the ground state $^2\Pi_{1/2}$.

Table 5 Frequencies (MHz), sensitivity coefficients, and reduced MEs (a.u.) for some K-doubling transitions in $\Pi_{1/2}$ state of the l-C_3H molecule.

$J\ F'p',\ Fp$	ω	Q_α	Q_μ	$\|\|D\|\|^2$
$\frac{1}{2}$ 1+, 0−	52.37	0.66(2)	1.7(2)	0.333
$\frac{1}{2}$ 0+, 1−	39.12	0.20(2)	1.9(2)	0.333
$\frac{1}{2}$ 1+, 1−	34.93	−0.02(2)	2.0(2)	0.667
$\frac{3}{2}$ 1−, 1+	85.55	0.65(2)	1.7(1)	0.166
$\frac{3}{2}$ 2−, 1+	78.60	0.55(2)	1.7(1)	0.033
$\frac{3}{2}$ 1−, 2+	75.23	0.43(2)	1.8(1)	0.033
$\frac{3}{2}$ 2−, 2+	68.29	0.30(2)	1.8(1)	0.299
$\frac{5}{2}$ 2+, 2−	107.19	0.95(2)	1.5(1)	0.132
$\frac{5}{2}$ 3+, 2−	98.97	0.89(2)	1.5(1)	0.009
$\frac{5}{2}$ 2+, 3−	98.83	0.82(2)	1.6(1)	0.009
$\frac{5}{2}$ 3+, 3−	90.61	0.75(2)	1.6(1)	0.188
$\frac{7}{2}$ 3−, 3+	112.38	1.63(2)	1.2(1)	0.105
$\frac{7}{2}$ 4−, 4+	96.07	1.56(2)	1.2(1)	0.136
$\frac{9}{2}$ 4+, 4−	95.75	3.22(4)	0.36(7)	0.086
$\frac{9}{2}$ 5+, 5−	79.63	3.45(4)	0.23(7)	0.105
$\frac{11}{2}$ 5−, 5+	52.81	9.1 (6)	−2.6 (3)	0.072
$\frac{11}{2}$ 6−, 6+	36.85	12.1 (6)	−4.1 (3)	0.085
$\frac{13}{2}$ 6−, 6+	20.25	− 34. (2)	19. (2)	0.062
$\frac{13}{2}$ 7−, 7+	36.06	− 18. (2)	11. (2)	0.071
$\frac{15}{2}$ 7+, 7−	126.59	−7.6 (2)	5.8 (4)	0.054
$\frac{15}{2}$ 8+, 8−	142.24	−6.5 (2)	5.3 (4)	0.061
$\frac{17}{2}$ 8−, 8+	268.76	−4.7 (1)	4.4(3)	0.047
$\frac{17}{2}$ 9−, 9+	284.25	−4.3 (1)	4.2(3)	0.053
$\frac{19}{2}$ 9+, 9−	448.75	−3.59(7)	3.8(3)	0.042
$\frac{19}{2}$ 10+, 10−	464.07	−3.39(7)	3.7(3)	0.046
$\frac{21}{2}$ 10−, 10+	668.02	−2.97(6)	3.5 (3)	0.038
$\frac{21}{2}$ 11−, 11+	683.18	−2.85(6)	3.4 (3)	0.041

It is clear that tunneling frequencies should strongly depend on the nuclear masses, and we can expect large sensitivity coefficients $Q_{\mu,\mathrm{tun}}$. They can be found using

Table 6 Frequencies (MHz), sensitivity coefficients, and reduced MEs (a.u.) for some K-doubling transitions in $\Pi_{3/2}$ state of the l-C_3H molecule.

$J\ F'p', Fp$	ω	Q_α	Q_μ	$\|\|D\|\|^2$
$\frac{3}{2}\ 1-, 1+$	5.61	−2.63(8)	3.2 (2)	1.493
$\frac{3}{2}\ 2-, 1+$	18.50	0.49(8)	1.7 (2)	0.299
$\frac{3}{2}\ 1-, 2+$	−7.30	5.28(8)	−0.6 (2)	0.299
$\frac{3}{2}\ 2-, 2+$	5.58	−2.63(8)	3.2 (2)	2.688
$\frac{5}{2}\ 2+, 2-$	22.24	−2.60(8)	3.2 (2)	1.186
$\frac{5}{2}\ 3+, 2-$	31.50	−1.35(8)	2.6 (2)	0.085
$\frac{5}{2}\ 2+, 3-$	12.88	−5.67(8)	4.6 (2)	0.085
$\frac{5}{2}\ 3+, 3-$	22.15	−2.60(8)	3.2 (2)	1.694
$\frac{7}{2}\ 3-, 3+$	54.92	−2.57(8)	3.2 (2)	0.943
$\frac{7}{2}\ 4-, 4+$	54.76	−2.57(8)	3.2 (2)	1.223
$\frac{9}{2}\ +-$	108.13	−2.50(8)	3.1 (2)	1.230
$\frac{11}{2}\ -+$	185.99	−2.46(8)	3.1 (2)	1.007
$\frac{39}{2}\ -+$	4266.17	−2.9 (1)	2.53(8)	0.224
$\frac{41}{2}\ +-$	4553.04	−3.5 (1)	2.42(5)	0.208
$\frac{43}{2}\ -+$	4663.43	−4.6 (2)	2.2 (1)	0.192
$\frac{45}{2}\ +-$	4377.16	−7.5 (2)	1.4 (3)	0.174
$\frac{47}{2}\ -+$	3097.96	−19.0 (4)	−2.3 (9)	0.149
$\frac{49}{2}\ -+$	909.06	132. (2)	53.(8)	0.103
$\frac{51}{2}\ -+$	19813.69	−3.11(5)	−1.6 (4)	0.116

the semi-classical Wentzel-Kramers-Brillouin (WKB) approximation. Following [77] we can write the ground state tunneling frequency in atomic units ($\hbar = |e| = m_e = 1$) as:

$$\omega_{\rm tun} \approx \frac{2E_0}{\pi}\, e^{-S}, \tag{30}$$

where S is the action over classically forbidden region and E_0 is the ground state vibrational energy calculated from the bottom of the well $U_{\rm min}$. If the barrier is high enough the harmonic approximation gives $2E_0 = \omega_\nu$, where ω_ν is the observed vibrational frequency. In this case Eq. (30) allows to find action S from experimentally known frequencies $\omega_{\rm tun}$ and ω_ν. For lower barriers we need to know the shape of the potential to estimate E_0. The examples of these two limiting cases are ammonia and hydronium, where tunneling frequencies are 0.8 cm^{-1} and 55 cm^{-1} respectively.

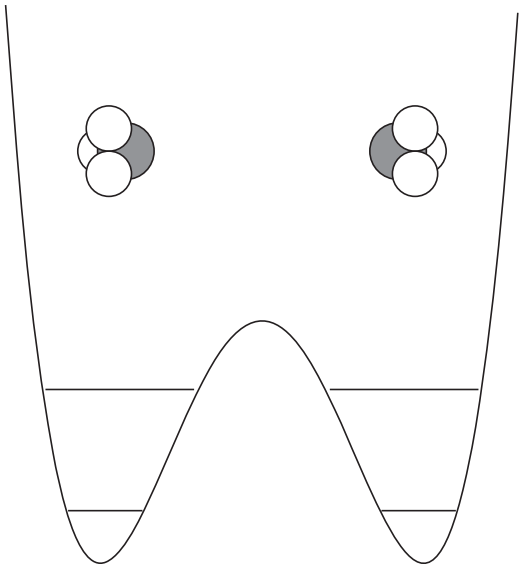

Figure 5 Potential for the tunneling (umbrella) mode of the NH_3 molecule. Two lowest vibrational levels lie below the barrier.

The action S depends on the tunneling mass, which in atomic units is proportional to μ^{-1}. Differentiating (30) over μ we get [78, 79]

$$Q_{\mu,\rm tun} \approx \frac{1+S}{2} + \frac{S\,E_0}{2(\Delta U - E_0)}\,, \tag{31}$$

where $\Delta U = U_{\rm max} - U_{\rm min}$ is the barrier hight. Numerical solution of the Schrödinger equation for realistic potentials agrees with this WKB expression within few percent for all molecules considered so far.

5.1 Ammonia

Equations (30), (31) show that sensitivity coefficient logarithmically depends on the tunneling frequency. For example, for the symmetric isotopologues of ammonia we get:

$$NH_3: \qquad \omega_{\rm tun} = 24\,{\rm GHz}, \quad Q_{\mu,\rm tun} = 4.5\,, \tag{32a}$$

$$ND_3: \qquad \omega_{\rm tun} = 1.6\,{\rm GHz}, \quad Q_{\mu,\rm tun} = 5.7\,. \tag{32b}$$

Such a weak dependence on the tunneling frequency limits possible values of the sensitivity coefficients for tunneling transitions in the microwave range: $Q_{\mu,\rm tun} \lesssim 8$. This is quite good, compared to the rotational sensitivity $Q_{\mu,\rm rot} \approx 1$, but smaller than the best sensitivities in linear molecules considered above.

Let us consider mixed tunneling-rotational transitions, where tunneling goes along with the change of the rotational quantum numbers. If we neglect interaction between tunneling and rotational degrees of freedom we can write approximate expressions for the frequency and the sensitivity of the mixed inversion-rotational transition:

$$\omega_{\rm mix} = \omega_r \pm \omega_{\rm tun}\,, \tag{33a}$$

$$Q_{\mu,{\rm mix}} = \frac{\omega_r}{\omega_{\rm mix}} \pm Q_{\mu,{\rm tun}}\frac{\omega_{\rm tun}}{\omega_{\rm mix}}\,. \tag{33b}$$

We are particularly interested in the case when the minus sign in (33) is realized and $\omega_{\rm mix} \ll \omega_{\rm tun}$. For this case the tunneling sensitivity is enhanced by the factor $\omega_{\rm tun}/\omega_{\rm mix} \gg 1$ and resultant sensitivity of the mixed transition is inversely proportional to the transition frequency $\omega_{\rm mix}$. Therefore, *for the mixed transitions we can have much higher sensitivities in the observable frequency range, then for the purely tunneling transitions.*

Another important advantage of the mixed transitions is that there are usually many of them each having different sensitivity. This means that we can have very good control on possible systematics and reliably estimate the accuracy of the results for μ-variation.

The mixed transitions can not be observed in the symmetric isotopologues of ammonia (32), but they are observed in the partly deuterated species NH_2D and NHD_2. Unfortunately, for both of them the tunneling frequency is much smaller then all rotational frequencies and sensitivities (33b) are not large [80]:

$$\begin{aligned} &{\rm NH_2D}: && 0.10 \le Q_{\mu,{\rm mix}} \le 1.61\,,\\ &{\rm NHD_2}: && 0.27 \le Q_{\mu,{\rm mix}} \le 1.54\,. \end{aligned} \tag{34}$$

Relatively small sensitivity coefficients for deuterated isotopologues of ammonia (34) and their low abundance does not allow to get strong limits on μ-variation, so we need to use tunneling ammonia line (32a). It was observed from the several objects with the redshifts about unity. Measuring radial velocities for rotational lines and for the ammonia tunneling line we have $\Delta Q = 3.5$ in Eq. (8), which is two orders of magnitude larger than for optical lines. Because of that the ammonia method allowed to place more stringent bounds on μ-variation than bounds, which follow from the optical spectra of the hydrogen molecule. However, recent observations of the molecules with mixed tunneling-rotational transitions provide even higher sensitivity to μ-variation.

5.2 Mixed tunneling-rotational transitions and effective Hamiltonians

Equations (33) show that high sensitivity mixed transitions are possible when tunneling frequency is of the same order of magnitude as rotational constants. However, in this case tunneling and rotational degrees of freedom start to interact and the accuracy of approximation (33) decreases. A much better approximation can be reached with the help of the effective Hamiltonians, which describe rotational and tunneling degrees of freedom and their interactions with each other. At present the state of the art effective Hamiltonians can include on the order of hundred parameters. These parameters are fitted to the experimentally known transitions and provide an accuracy on the ppm scale, or better.

When such Hamiltonians are used to find sensitivity coefficients Q_μ we need to know how all the parameters depend on μ. It was shown in [25] that this can usually be done only within an accuracy of a few percent. The final accuracy for the large Q-factors is somewhat lower because of the instability of Eq. (33b). Because of that we need not complex effective Hamiltonians but their simplified versions with considerably smaller numbers of fitting parameters can be used instead.

5.3 Hydronium and peroxide

Let us start with hydronium molecule H_3O^+ [81]. This molecule is a symmetric top. It is similar to ammonia, but flatter. Tunneling frequency is almost 50 times larger and comparable to rotational intervals. The tunneling umbrella mode does not change the symmetry and does not contribute to the angular momentum of the molecule. Because of that the tunneling-rotational interaction is reduced to the centrifugal corrections to the tunneling frequency [82].

The tunneling-rotational spectrum of hydronium is shown in Fig. 6. It consists of the J ladders for each quantum number K, where K is projection of the angular momentum on the molecular axis. Due to the tunneling each rotational level is split in two states with different parity p. For $K = 0$ the permutation symmetry of the hydrogen nuclei allows only one of these levels, while for $K > 0$ both levels are present.

In Fig. 6 we see four mixed transitions with frequencies around 300 GHz, which is few times smaller than the tunneling frequency that is about 1.6 THz. Table 7 shows that these transitions have enhanced sensitivity to μ variation ($Q_{\mu,{\rm tun}} = 2.0 \pm 0.1$). Those transitions, whose

frequencies decrease when tunneling frequency increases have negative sensitivity coefficients Q_μ. We conclude that hydronium has several mixed transitions with sensitivities of both signs and the maximum ΔQ_μ is around 10. Other isotopologues of hydronium have even higher sensitivities [79], but up to now they have not been observed in the interstellar medium.

Another molecule where tunneling frequency is comparable to rotational constants, but tunneling-rotational interaction is rather weak, is peroxide H_2O_2 [83, 84]. In equilibrium geometry H_2O_2 is not flat; the angle 2γ between two HOO planes is close to 113°. Two flat configurations correspond to local maxima of potential energy; the potential barrier for *trans* configuration ($2\gamma = \pi$) is significantly lower, than for *cis* configuration ($\gamma = 0$): $U_\pi \approx 400$ cm^{-1} and $U_0 \approx 2500$ cm^{-1}. To a first approximation one can neglect the tunneling through the higher barrier. In this model peroxide is described by a slightly asymmetric oblate top with inversion tunneling mode, similar to ammonia and hydronium.

The sensitivity coefficients for the mixed transitions in peroxide were calculated in [86]. Results of these calculations are shown in Table 8. Molecular states are labeled with the rotational quantum numbers J, K_A, and K_C and the tunneling quantum number τ [83]. Transitions with the frequencies below 100 GHz were found to

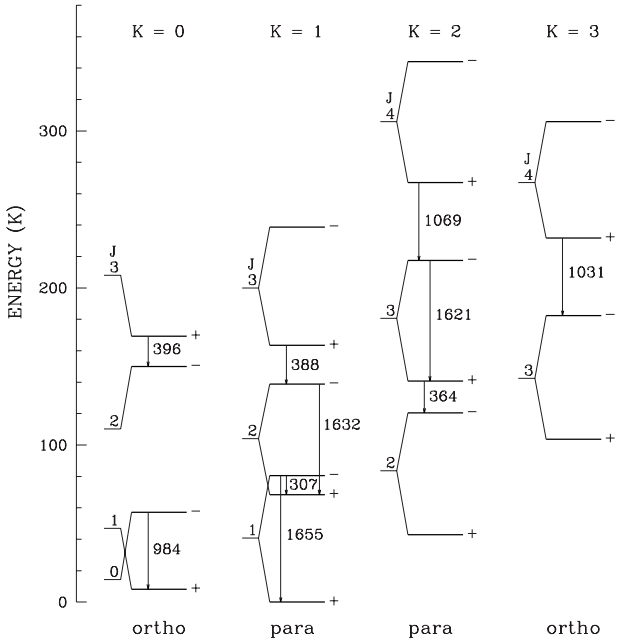

Figure 6 Tunneling-rotational spectrum of H_3O^+ molecule. Several low-frequency tunneling and mixed transitions are marked with vertical arrows. Their frequencies are shown in GHz.

Table 7 Sensitivities of the low frequency mixed inversion-rotational transitions in hydronium H_3O^+. Molecular states are labeled with quantum numbers J^p_K.

Transition		Frequency (MHz)		
Upper	Lower	Theory	Exper.	Q_μ
1^-_1	2^+_1	307072	307192.4	6.4(5)
3^+_2	2^-_2	365046	364797.4	−3.5(5)
3^+_1	2^-_1	389160	388458.6	−3.1(4)
3^+_0	2^-_0	397198	396272.4	−3.0(4)
0^-_0	1^+_0	984690	984711.9	2.7(2)
4^+_3	3^-_3	1031664	1031293.7	−0.6(2)
4^+_2	3^-_2	1071154	1069826.6	−0.5(2)
3^-_2	3^+_2	1621326	1621739.0	2.0(1)
2^-_1	2^+_1	1631880	1632091.0	2.0(1)
1^-_1	1^+_1	1655832	1655833.9	2.0(1)

Table 8 Numerical calculation of the Q-factors for low frequency mixed transitions in peroxide H_2O_2 using effective Hamiltonian. Experimental frequencies are taken from JPL Catalogue [61]. $E_{\rm up}$ is upper state energy in Kelvin.

$J_{K_A,K_C}(\tau)$			ω (MHz)		
upper	lower	$E_{\rm up}$ (K)	theory	exper.	Q_μ
Transitions below 100 GHz					
$0_{0,0}(3)$	$1_{1,0}(1)$	17	14818.8	14829.1	+36.5(2.9)
$2_{1,1}(1)$	$1_{0,1}(3)$	21	37537.0	37518.28	−13.0(1.2)
$1_{0,1}(3)$	$1_{1,1}(1)$	19	67234.5	67245.7	+8.8(6)
$2_{0,2}(3)$	$2_{1,2}(1)$	24	68365.3	68385.0	+8.7(6)
$3_{0,3}(3)$	$3_{1,3}(1)$	31	70057.4	70090.2	+8.5(6)
$4_{0,4}(3)$	$4_{1,4}(1)$	41	72306.0	72356.4	+8.3(6)
$5_{0,5}(3)$	$5_{1,5}(1)$	53	75104.6	75177.4	+8.0(6)
$6_{0,6}(3)$	$6_{1,6}(1)$	68	78444.7	78545.4	+7.7(6)
$3_{1,2}(1)$	$2_{0,2}(3)$	28	90399.8	90365.51	−4.8(5)
Transitions observed from ISM in [85]					
$3_{0,3}(3)$	$2_{1,1}(1)$	31	219163.2	219166.9	+3.4(2)
$6_{1,5}(1)$	$5_{0,5}(3)$	66	252063.6	251914.68	−1.1(2)
$4_{0,4}(3)$	$3_{1,2}(1)$	41	268963.7	268961.2	+3.0(2)
$5_{0,5}(3)$	$4_{1,3}(1)$	53	318237.7	318222.5	+2.7(1)

have rather high sensitivities of both signs. Several transitions of peroxide were recently observed from interstellar medium (ISM) in [85]. These transitions have higher frequencies and smaller sensitivities to μ-variation. Nevertheless, even for these transitions the maximum value of ΔQ_μ is about 4.5.

5.4 Molecules with hindered rotation: methanol and methylamine

Hindered rotation is one of the examples of the large amplitude internal motions in non rigid molecules. In the discussion of the peroxide molecule in the previous subsection, we neglected the tunneling through the higher *cis* barrier. For the excited vibrational states tunneling through both barriers can take place leading to the hindered rotation of one HO group in respect to another. Many molecules which include CH_3 group have three equivalent minima at 120° to each other. Hindered rotation in such molecules can take place already for the ground vibrational state. When the tunneling frequencies are comparable to the rotational ones, such molecules have very rich microwave spectra with a large number of mixed transitions. Another distinctive feature of these molecules is strong interaction between the internal (hindered) and overall rotations. One of the simplest molecules of this type is methanol CH_3OH.

The basic theory of the non-rigid tops with internal rotation was established in the 1950s [87, 88] and the main features of the methanol spectrum were explained. Later on the theory was refined many times and currently there is a very impressive agreement between the theory and experiment [89–92].

The sensitivity coefficients to the μ-variation for methanol microwave transitions were calculated independently in [93, 94] and in [25]. The first group used the state of the art effective Hamiltonian [91], which included 120 fitting parameters. The second group used a much simpler model [95]. The rotational part $H_{\rm rot}$ was that of the slightly asymmetric top and included the rotational constants A, B, and C ($A \approx B$). The hindered rotation was described by the Hamiltonian

$$H_{\rm hr} = -F\frac{{\rm d}^2}{{\rm d}\omega^2} + \frac{V_3}{2}(1-\cos 3\omega)\ , \qquad (35)$$

where the kinetic coefficient F was proportional to μ and the electronic potential V_3 was independent on μ. The angle ω described position of the OH group in respect to the CH_3 top. This model did not include centrifugal distortions. The interaction of the internal rotation with the overall rotation was described by a single parameter D, which scaled linearly with μ [87]. Altogether this model had 6 parameters.

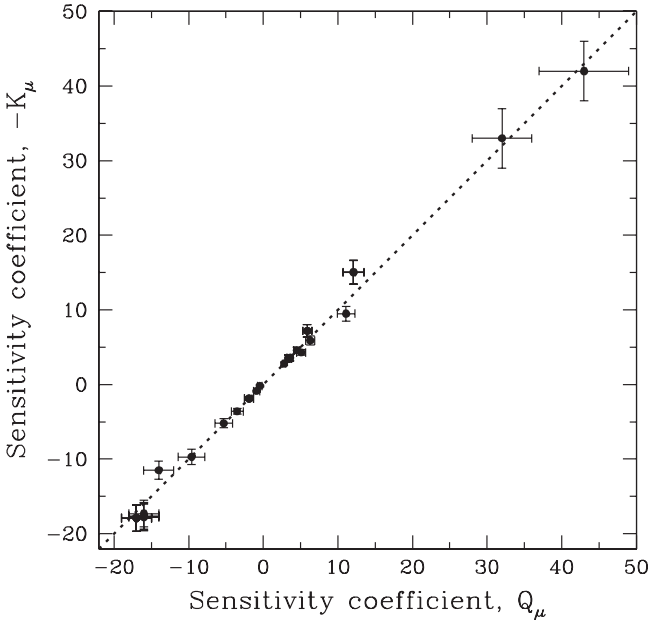

Figure 7 Comparison of the sensitivity coefficients for CH_3OH from [93] and [25]. The former used the sensitivity coefficients K_μ defined as $K_\mu = -Q_\mu$. This corresponds to the different definition of the mass ratio: $m_{\rm p}/m_{\rm e}$ instead of $m_{\rm e}/m_{\rm p}$, which is used in the present review.

Both effective Hamiltonians were diagonalized for several sets of parameters, which correspond to an increased and decreased μ and the sensitivity coefficients were found by the numerical differentiation. The comparison of the two calculations is given in Fig. 7. We see that in spite of a significant difference in complexity of the models the results are in good agreement and of the comparable accuracy. As we discussed above, the latter is mostly determined by ambiguity in the μ-scaling of model parameters.

The sensitivity coefficients for the mixed transitions in methanol span from −17 to +43, which corresponds to $|\Delta Q_\mu| \sim 60$. This is more than an order of magnitude larger than in ammonia method. Moreover, in methanol we have a large number of strong lines with different sensitivities and can effectively control possible systematic effects. Until very recently methanol was observed only at small redshifts, but in 2011 it was first detected in the microwave survey towards the object PKS 1830-211 at redshift $z = 0.89$ [96]. This means that at present methanol can be used as a very

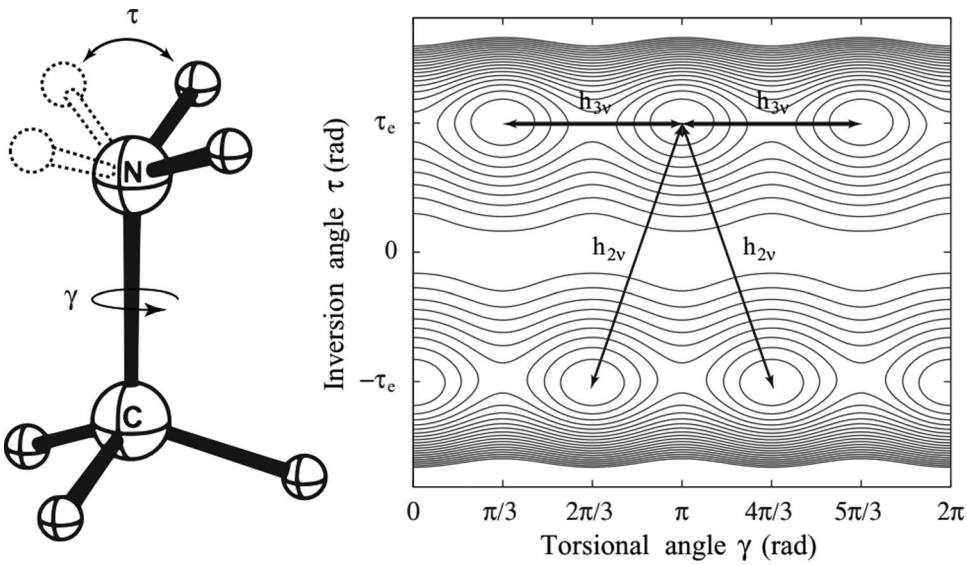

Figure 8 Schematic representation of methylamine and variation of the potential energy of methylamine as function of the relative rotation γ of the CH_3 group with respect to the amine group about the CN bond and the angle τ of the two hydrogen atoms of the NH_2 group with respect to the CN bond. The two large amplitude motions, corresponding to inversion $h_{2\nu}$ and hindered rotation $h_{3\nu}$ are schematically indicated by the arrows. Note that inversion of the NH_2 group is accompanied by a $\pi/3$ rotation about the CN bond of the CH_3 group with respect to the amine group.

sensitive tool to probe μ-variation on a cosmological timescale [23, 97].

In the same survey [96], a large number of rather complex molecules were detected for the first time at high redshift. In particular, the list includes methylamine — yet another molecule with tunneling motion. In contrast to all previously discussed molecules, methylamine has two tunneling modes. First is hindered rotation of the NH_2 around CH_3 top, which is similar to that in methanol. Second is a wagging mode when the NH_2 group flips over to the other side (see Fig. 8). Both modes contribute to the angular momentum of the molecule and, therefore, strongly interact with the overall rotation.

The spectrum of methylamine is also very rich. The effective Hamiltonian must include both tunneling motions and their interactions with each other and with the overall rotation. Therefore, even the simplest form of this Hamiltonian is quite complex and we will not discuss it here. Calculations of the sensitivity coefficients were recently done in [98]. It was found that they lie in the range $-24 \leq Q_\mu \leq 19$. However, the lines, which were observed in [96] at $z = 0.89$ have sensitivities close to 1. Up to now neither of the more sensitive lines of methylamine has been observed at high redshifts.

There are several other molecules with mixed tunneling-rotational spectra, for example N_2H_4 and CH_3SH. The former has three tunneling modes which strongly interact with rotation. Thus, we should expect very complex spectrum. This molecule is predicted to form in Jupiter's and Titan's atmospheres [99, 100]. The latter is similar to methanol and exhibits hindered rotation and complex spectrum [101]. Effective Hamiltonians for many of these molecules are known, but no other calculations of the sensitivity coefficients have been done so far (preliminary results for CH_3SH show that there are transitions with high sensitivities of both signs). If any new sufficiently low frequency mixed transitions are observed from the interstellar medium, it is possible to calculate respective sensitivity coefficients using the methods outlined in this section.

6 Summary and conclusions

As we discussed in the previous sections the constraints on the possible variation of fundamental constants are an efficient method of testing the equivalence principle which is a basic assumption of General Relativity. These constraints can be derived from a wide variety of atomic and molecular transitions observed in laboratory, solar and extra solar systems, and at very early cosmological epochs up to a redshift of order $z \sim 5 - 6$ where molecular and atomic transitions have been recently detected and observed with a sufficiently high spectral resolution [14, 15]. Radio astronomical observations of the NH_3 molecule in two distant galaxies provide tight constraints

at the $\Delta\mu/\mu < 1 \times 10^{-6}$ level at $z = 0.89$ [102] and $z = 0.69$ [13]. Even deeper bounds were deduced from observations of the CH_3OH molecule in the $z = 0.89$ galaxy: $\Delta\mu/\mu < 3 \times 10^{-7}$ [97], and $\Delta\mu/\mu < 1 \times 10^{-7}$ [23].

To probe α and μ at the level of 10^{-8} or 10^{-9}, at least two main requirements should be fulfilled: (*i*) increasing precision of the laboratory measurements of the rest frame frequencies of the most sensitive molecular transitions discussed in this review, and (*ii*) increasing sensitivity and spectral resolution of astronomical observations.

The most promising molecular transitions are those of a mixed nature, where there are two, or more, competing contributions to the transition energy. We get strong enhancement of the sensitivity to the variation of the fundamental constants when the resultant transition frequency is much smaller than individual contributions. This happens, for example, for some mixed tunneling-rotational transitions. Diatomic radicals give another example, where spin-orbit interaction is competing with Coriolis interaction. As a result we have strong enhancement of the sensitivity coefficients for the Λ-doublet transitions. There are other known examples, which are more relevant for the laboratory experiments [103,104]. It is possible that more examples will be found both for the laboratory and astrophysical studies. The methods described in this review allow us to calculate sensitivity coefficients for any microwave and submillimeter molecular transitions of interest.

Mikhail G. Kozlov received his Ph.D. degree in Physics 1982 from the Petersburg Nuclear Physics Institute (PNPI) in Russia where he is currently a Leading Research Scientist. He is also a Professor of Physics at St. Petersburg Electrotechnical University. Kozlov's research interests include atomic and molecular theory, fundamental symmetries, and fundamental constants.

Sergei A. Levshakov received his Ph.D. degree in Physics 1982 from the Physical-Technical Institute (PTI), St. Petersburg (Russia) where he is currently a Leading Research Scientist. He is also a Professor of Physics at St. Petersburg Electrotechnical University. Levshakov's research interests include astrophysics and space science, atomic and molecular spectroscopy, chemical evolution and the origin of the elements, and data analysis.

References

[1] R. P. Feynman, QED: the Strange Theory of Light and Matter (Princeton, NJ, Princeton Univ. Press, 1985), p. 129.
[2] E. A. Milne, Proc. Roy. Soc. A. **158**, 324 (1937).
[3] P. A. M. Dirac, Nature **139**, 323 (1937).
[4] A. Cingöz et al., Phys. Rev. Lett. **98**, 040801 (2007).
[5] Yu. V. Petrov et al., Phys. Rev. C **74**, 064610 (2006).
[6] T. Rosenband et al., Science **319**, 1808 (2008).
[7] A. Shelkovnikov, R. J. Butcher, C. Chardonnet, and A. Ami-Klein, Phys. Rev. Lett. **100**, 150801 (2008).
[8] S. Blatt et al., Phys. Rev. Lett. **100**, 140801 (2008).
[9] M. C. Ferreira, M. D. Julião, C. J. A. P. Martins, and A. M. R. V. L. Monteiro, Phys. Rev. D **86**, 125025 (2012).
[10] V. V. Flambaum, Int. J. Mod. Phys. A **22**, 4937 (2007).
[11] P. Molaro, D. Reimers, I. I. Agafonova, and S. A. Levshakov, Eur. Phys. J. Special Topics **163**, 173 (2008).
[12] I. I. Agafonova, P. Molaro, S. A. Levshakov, and J. L. Hou, Astron. Astrophys. **529**, A28 (2011).
[13] N. Kanekar, Astrophys. J. **728**, L12 (2011).
[14] S. A. Levshakov et al., Astron. Astrophys. **540**, L9 (2012).
[15] L. Lentati et al., Mon. Not. R. Astron. Soc. **430**, 2454 (2013).
[16] S. J. Landau, M. E. Mosquera, C. G. Scóccola, and H. Vucetich, Phys. Rev. D **78**, 083527 (2008).
[17] C. J. A. P. Martins et al., Phys. Rev. D **82**, 023532 (2010).
[18] M. Nakashima, K. Ichikawa, R. Nagata, and J. Yokoyama, J. Cos. Astropart. Phys. **01**, 030 (2010).
[19] V. V. Flambaum and E. V. Shuryak, Phys. Rev. D **65**, 103503 (2002).
[20] A. Coc et al., Phys. Rev. D **86**, 043529 (2012).

[21] J. K. Webb et al., Phys. Rev. Lett. **107**, 191101 (2011).
[22] H. Rahmani et al., 2012, Mon. Not. R. Aastron. Soc. **425**, 556 (2012).
[23] J. Bagdonaite et al., Science **339**, 46 (2013).
[24] S. A. Levshakov et al., 2010, Astron. Astrophys. **512**, A44 (2010).
[25] S. A. Levshakov, M. G. Kozlov, and D. Reimers, Astrophys. J. **738**, 26 (2011).
[26] S. Ellingsen, M. Voronkov, and S. Breen, Phys. Rev. Lett. **107**, 270801 (2011).
[27] T. Damour, 2012, Class. Quant. Gravity **29**, 184001 (2012).
[28] J.-P. Uzan, Living Reviews in Relativity **14**, 2 (2011).
[29] M. Raidal et al., Eur. Phys. J. C **57**, 13 (2008).
[30] T. Fukuyama, Int. J. Mod. Phys. A **27**, 30015 (2012).
[31] V. V. Fritzsch, Uspekhi Fiz. Nauk **52**, 359 (2009).
[32] V. A. Dzuba, V. V. Flambaum, and J. K. Webb, Phys. Rev. Lett. **82**, 888 (1999).
[33] V. A. Dzuba, V. V. Flambaum, and J. K. Webb, Phys. Rev. A **59**, 230 (1999).
[34] J. C. Berengut et al., in: From Varying Couplings to Fundamental Physics, edited by C. Martins and P. Molaro (Springer-Verlag, Berlin, 2011), p. 9.
[35] D. A. Varshalovich and S. A. Levshakov, J. Exp. Theor. Phys. **58**, 231 (1993).
[36] V. V. Meshkov, A. V. Stolyarov, A. V. Ivanchik, and D. A. Varshalovich, J. Exper. Theor. Phys. Lett. **83**, 303 (2006).
[37] W. Ubachs, R. Buning, K. Eikema, and E. Reinhold, J. Mol. Spectrosc. **241**, 155 (2007).
[38] E. J. Salumbides et al., Phys. Rev. A **86**, 022510 (2012).
[39] S. G. Porsev et al., Phys. Rev. A **76**, 052507 (2007).
[40] G. Nave and S. Johansson, Astrophys. J. Suppl. **204**, 1 (2013).
[41] S. A. Levshakov, M. Centurión, P. Molaro, and S. D'Odorico, Astron. Astrophys. **434**, 827 (2005).
[42] K. Griest et al., Astrophys. J. **708**, 158 (2010).
[43] J. B. Whitmore, M. T. Murphy, and K. Griest, Astrophys. J. **723**, 89 (2010).
[44] I. I. Agafonova et al., Astron. Astrophys. **552**, A83 (2013).
[45] E. J. Salumbides et al., Phys. Rev. Lett. **101**, 223001 (2008).
[46] P. Noterdaeme et al., Astron. Astrophys. **523**, A80 (2010).
[47] S. A. Levshakov, M. Dessauges-Zavadsky, S. D'Odorico, and P. Molaro, Mon. Not. R. Astron. Soc. **333**, 373 (2002).
[48] M. Wendt and P. Molaro, Astron. Astrophys. **541**, A69 (2012).
[49] M. G. Kozlov et al., Phys. Rev. A **77**, 032119 (2008).
[50] S. A. Levshakov et al., Astron. Astrophys. **479**, 719 (2008).
[51] S. G. Kukolich, Phys. Rev. **156**, 83 (1967).
[52] E. R. Hudson, H. J. Lewandowski, B. C. Sawyer, and J. Ye, Phys. Rev. Lett. **96**, 143004 (2006).
[53] J. N. Chengalur and N. Kanekar, Phys. Rev. Lett. **91**, 241302 (2003).
[54] J. Darling, Phys. Rev. Lett. **91**, 011301 (2003).
[55] M. G. Kozlov, Phys. Rev. A **80**, 022118 (2009).
[56] A. J. de Nijs, W. Ubachs, W., and H. L. Bethlem, Phys. Rev. A **86**, 032501 (2012).
[57] C. M. Persson et al., Astron. Astrophys. **543**, A145 (2012).
[58] K. Beloy et al., Phys. Rev. A **83**, 062514 (2011).
[59] J. M. Brown and A. Carrington, Rotational Spectroscopy of Diatomic Molecules (Cambridge University Press, Cabmridge, 2003).
[60] F. J. Lovas et al., Diatomic Spectral Database (2005) (http://www.physics.nist.gov/PhysRefData/ MolSpec/Diatomic/index.html)
[61] H. M. Pickett et al., J. Quant. Spectrosc. Rad. Transfer **60**, 883 (1998) (http://spec.jpl.nasa.gov).
[62] H. S. P. Müller, F. Schlöder, J. Stutzki, and Winnewisser, J. Mol. Struct. **742**, 215 (2005) (http://www.astro.uni-koeln.de/site/vorhersagen).
[63] W. L. Meerts and A. Dymanus, J. Mol. Spec. **44**, 320 (1972).
[64] J. M. Brown, G. A. Colbourn, J. K. G. Watson, and F. D. Wayne, J. Mol. Spec. **74**, 294 (1979).
[65] J. M. Brown and A. J. Merer, J. Mol. Spec. **74**, 488 (1979).
[66] S. Davidson, K. M. Evenson, and J. M. Brown, Astrophys. J. **546**, 330 (2001).
[67] M. A. Martin-Drumel et al., Chem. Phys. Lett. **550**, 8 (2012).
[68] K. Kawaguchi and T. Amano, J. Chem. Phys. **88**, 4584 (1988).
[69] H. Hübers, K. M. Evenson, C. Hill, and J. M. Brown, J. Chem. Phys. **131**, 034311 (2009).
[70] R. Renner, Zeitschrift für Physik **92**, 172 (1934).
[71] J. T. Hougen, J. Chem. Phys. **36**, 519 (1962).
[72] M. G. Kozlov, Phys. Rev. A **87**, 032104 (2013).
[73] M. Perić, M. Mladenović, K. Tomić, and C. M. Marian, J. Chem. Phys. **118**, 4444 (2003).
[74] S. Yamamoto et al., Astrophys. J. **348**, 363 (1990).
[75] M. Kanada, S. Yamamoto, S. Saito, and Y. Osamura, J. Chem. Phys. **104**, 2192 (1996).
[76] M. Caris et al., J. Mol. Spect. **253**, 99 (2009).
[77] L. D. Landau and E. M. Lifshitz, Quantum mechanics (Oxford, Pergamon, 1977).
[78] V. V. Flambaum and M. G. Kozlov, Phys. Rev. Lett. **98**, 240801 (2007).
[79] M. G. Kozlov, S. G. Porsev, and D. Reimers, Phys. Rev. A **83**, 052123 (2011).
[80] M. G. Kozlov, A. V. Lapinov, and S. A. Levshakov, J. Phys. B **43**, 074003 (2010).
[81] M. G. Kozlov and S. A. Levshakov, Astrophys. J. **726**, 65 (2011).
[82] S. Yu, B. J. Drouin, J. C. Pearson, and H. M. Pickett, Astrophys. J. Suppl. **180**, 119 (2009).
[83] J. T. Hougen, Canadian J. Phys. **62**, 1392 (1984).
[84] F. Masset et al., J. Phys. France **49**, 1901 (1988).
[85] P. Bergman et al., Astron. Astrophys. **531**, L8 (2011).
[86] M. G. Kozlov, Phys. Rev. A **84**, 042120 (2011).
[87] C. C. Lin and J. D. Swalen, Rev. Mod. Phys. **31**, 841 (1959).
[88] D. R. Herschbach, J. Chem. Phys. **31**, 91 (1959).

[89] T. Anderson, F. De Lucia, and E. Herbst, Astrophys. J. Suppl. **72**, 797 (1990).
[90] H. S. P. Müller, L. H. Xu, and F. van der Tak, J. Mol. Struc. **795**, 114 (2006).
[91] L. Xu et al., J. Mol. Spec. **251**, 305 (2008).
[92] I. Kleiner, J. Mol. Spec. **260**, 1 (2010).
[93] P. Jansen et al., Phys. Rev. Lett. **106**, 100801 (2011).
[94] P. Jansen et al., Phys. Rev. A **84**, 062505 (2011).
[95] D. Rabli and D. R. Flower, Mon. Not. R. Astron. Soc. **403**, 2033 (2010).
[96] S. Muller et al., Astron. Astrophys. **535**, A103 (2011).
[97] S. P. Ellingsen, M. A. Voronkov, S. L. Breen, and J. E. J. Lovell, Astrophys. J. **747**, 7 (2012).
[98] V. V. Ilyushin et al., Phys. Rev. A **85**, 032505 (2012).
[99] J. I. Moses, A. D. Sperier, and T. C. Keane, Bull. Am. Astron. Soc. **40**, 459 (2008).
[100] G. P. Smith, Bull. Am. Astron. Soc. **42**, 970 (2010).
[101] F. L. Bettens et al., Astrophys. J. **510**, 789 (1999).
[102] C. Henkel et al., Astron. Astrophys. **500**, 725 (2009).
[103] C. Chin, V. V. Flambaum, and M. G. Kozlov, New J. Phys. **11**, 055048 (2009).
[104] H. L. Bethlem and W. Ubachs, Faraday Discussions **142**, 25 (2009).